Predictive modeling of self-catalyzed III-V nanowire growth

Frank Glas,* Mohammed Reda Ramdani, Gilles Patriarche, and Jean-Christophe Harmand
CNRS - Laboratoire de Photonique et de Nanostructures, Route de Nozay, 91460 Marcoussis, France
(Received 27 May 2013; revised manuscript received 27 August 2013; published 8 November 2013)

We develop a quantitative model of the self-catalyzed vapor-liquid-solid growth of GaAs nanowires, that depends on only a few *a priori* unknown physical parameters. The model is based on the sole consideration of the As species and incorporates all relevant mechanisms of exchange of As between the vapor, liquid, and solid phases, namely direct impingement of molecules on the droplet, their re-emission by the neighboring surfaces, evaporation from the droplet, and nucleation at the solid-liquid interface. It reproduces quantitatively all salient features of our experimental study, namely the variations of nanowire growth rate with As flux, temperature, and nanowire radius. From these optimized fits, we extract a complete set of model parameters, in particular the nucleus edge energy. We also determine quantities so far inaccessible to experiment, such as the As concentration in the droplet (about 1%), supersaturation of the liquid, and nucleation barrier, for individual nanowires. The model can then be used to predict the growth rate (and all quantities of interest) for an arbitrary GaAs nanowire of given geometry in arbitrary growth conditions, including conditions not yet explored experimentally, provided the fraction of the As flux re-emitted by its environment is known. Although largely ignoring group III elements, our model captures most of the physics of self-catalyzed nanowire growth.

DOI: 10.1103/PhysRevB.88.195304 PACS number(s): 81.10.Aj, 81.07.Gf, 81.05.Ea, 82.60.Nh

I. INTRODUCTION

Free-standing nanowires (NWs), with diameters of a few tens of nanometers and lengths up to several micrometers, are nowadays commonly fabricated from a large range of semiconductor materials. Most NWs, and in particular those of As and P-based III-V compounds, are obtained via the vapor-liquid-solid (VLS) method: Metal catalyst nanoparticles are first deposited or formed on a substrate; atoms are then fed from a vapor phase to the solid NW through this droplet, which remains liquid at the apex of the NW during growth.

Growth catalyzed by a foreign metal (gold in particular) is attractive, especially in terms of the control of the diameter and position of the NWs, and of the variety of materials and heterostructures that can be fabricated.[1–3] However, in the last few years, research on self-catalyzed III-V NW growth, whereby the liquid catalyst droplet contains only the group III constituent of the NW plus a small amount of its group V constituent, has developed rapidly. Work has concentrated on GaAs NWs grown by molecular beam epitaxy (MBE),[4–15] possibly with heterostructures,[15–17] although InP,[18] InAs,[19] and alloys[15,20] have also been grown this way. Self-catalyzed growth presents several advantages. Since the catalyst is made of the same elements as the NW, the risk of introducing unwanted impurities in the NW during growth is much reduced. Moreover, the crystal structure of the GaAs NWs is predominantly zinc blende (ZB)[7,10–12,15] (as opposed to the more or less random mixture of wurtzite and ZB structures that dominates in Au-catalyzed growth) and a regime where the growth rate of the NW is independent of its length may be attained,[4–6,15] which facilitates the control of axial heterostructures.

Quite generally, and despite substantial progress in recent years, the level at which even the most basic properties of the NWs (such as geometry, crystal structure, or doping) are controlled is still far from optimal. Most of these properties are determined right at the formation of the NWs. The applicability of NWs thus depends intimately on an understanding and control of the basic growth mechanisms governing their formation. A key element in this respect is the ability to model growth quantitatively. Surely much progress has been made in this field over the last decade.[21–33] However, the coexistence of three phases in VLS, the multiplicity of material pathways, and the fact that when a foreign catalyst is employed the liquid droplet is at least a ternary liquid (catalyst, group III, group V), make accurate modeling very tricky. Actually, with one exception,[33] all models published so far have considered only a single NW constituent, which is, explicitly or implicitly, the group III element. This approach, adapted from the standard models of noncatalyzed growth of III-V materials under an excess of group V element, is unsatisfactory. Several observations indeed point to the necessity of taking into account the group V constituent, in particular the influence of the group V flux on the growth rate[23,34–39] and crystal structure[34,36,40–43] of the NWs and on nucleation statistics.[44] Although steps have been made toward a more comprehensive modeling, such as the calculation of the chemical potential of the (Au, III, V) ternary liquids,[45] much remains to be done in this respect. Accordingly, by confronting models and experiments, only a limited number of quantities have been estimated, mainly diffusion lengths for group III atoms[9,21,24,26,39,46] and supersaturation of the parent phases.[21,23,27,31,39,44]

As regards modeling, self-catalyzed growth presents a clear advantage. When a binary NW is grown, the droplet, whose properties and state are determining in VLS growth, contains only two elements. Such (III, V) liquids have been widely used in the past for liquid phase epitaxy and their thermodynamic properties, as well as those of the vapors of the group III and group V species, are tabulated.[47] Because of the low solubilities of group V elements (other than Sb) in group III liquids, the droplet is mainly made of group III atoms in which a small concentration of group V (as yet unknown but estimated to be of the order of 1%[44,45]) is dissolved. The state of the bulk liquid is fully defined by its temperature and a single atomic concentration, for instance that of the group V constituent.

We develop our model for GaAs NWs grown by MBE and confront it to series of experiments where one of the parameters controlling growth, either the As flux or the temperature, is varied systematically.[15] We limit ourselves to NWs whose diameters remain constant during growth, which strongly suggests that the volume of the droplet, and hence the number of Ga atoms that it contains, change little. On the other hand, changing the As concentration in the liquid may widely modify the growth rate, with very little effect on its volume. Albeit small, the As concentration is thus essential for growth. One of the most striking features of self-catalyzed GaAs NW growth is indeed that the growth rate varies quasilinearly with the As beam flux over a large range of the latter, whereas it is more or less independent of the Ga beam flux.[4,6,8,12] Finally, we recently demonstrated that, at least in our growth conditions, surface diffusion of As species provides at most a minor contribution to self-catalyzed NW growth[15] (whereas diffusion might be of major import for Ga). Diffusion introduces much complication in NW growth modeling, since the diffusion fluxes toward the droplet depend, and at the same time partly determine, the composition and volume of the latter.[33,48] These considerations all lead to our proposal of a fairly simple model whereby, provided the group III flux is sufficient for the droplet to survive with a constant volume, growth under given conditions (temperature, fluxes) is fully determined by the sole group V element.

To summarize, we focus on the catalyst droplet and claim that the key point is the determination of the small amount of As that it contains. Indeed, as will be detailed shortly, addition of As to the droplet is determined (albeit not straightforwardly) by the flux impinging on the sample, by the droplet geometry and possibly by the NW environment, whereas removal of As from the droplet, via nucleation and growth of new solid monolayers (MLs) and evaporation, is determined (in addition to geometry) by the As concentration in the droplet and by temperature. Hence, if geometry and growth conditions are given, the As concentration in the droplet entirely determines growth.

This "As-only" approach is not exclusive of more elaborate models taking into account both group V and group III elements. Such a model has recently been developed.[33] It will prove essential, for instance, in describing the transient stages of growth or in understanding how the group III flux to the droplet may adapt to balance the As flux incorporated in the NW while maintaining a constant drop volume. However, the complexity of this model and the fact that it involves many unknown quantities makes it difficult to use for deriving values of the most important and basic material and growth parameters (to be specified below) or for predicting the outcome of growth experiments, which are our main aims.

II. MODEL

A. Introduction

Our As-only model couples group V material balance with nucleation at the liquid-solid interface. We consider MBE growth at temperature T and under a known flux of As. To be specific and to compare our predictions with experiments, we develop the model for GaAs NWs growing along a ZB $\langle 111 \rangle$ direction, but it could easily be adapted to other cases where the same hypotheses about the roles of group V and group III atoms would hold.

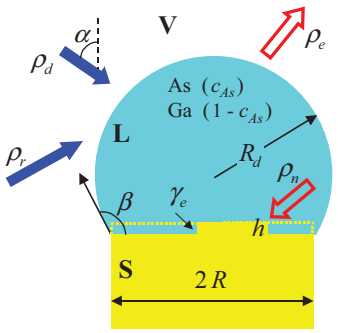

FIG. 1. (Color online) Schematics of self-catalyzed VLS growth of GaAs nanowires. The As currents that feed the (Ga, As) droplet of composition c_{As} (ρ_d from direct beam and ρ_r re-emitted by environment) are schematized by full blue arrows and those that deplete it (evaporation ρ_e and solid nucleation and growth ρ_n) by empty red arrows. Only ρ_d is directional, due to As_4 beam incident at angle α. The system geometry is defined by NW radius R, droplet radius R_d, and contact angle β. The edge of the solid nucleus has monolayer height h and effective energy γ_e.

The geometry is illustrated in Fig. 1. A NW of radius R grows perpendicularly to the substrate. A droplet in the shape of a spherical cap of radius R_d sits at the top of the NW, with contact angle $\beta \geqslant \pi/2$. Appendix A 3 recalls the relations between β, R, R_d, and the surface S_d and volume V_d of the droplet. The direct beam of As_4 molecules is inclined at an angle α with respect to the substrate normal and the corresponding *atomic* flux is J_d. In line with our experiments,[15] we assume that there is no radial growth (R remains constant).

During growth, several processes continually add As atoms to the droplet or remove As from it. Namely, As is added to the droplet by the direct beam and by re-emission from the nearby surfaces (see below), and removed by NW growth and by evaporation. The crucial differences between our As-only model of self-catalyzed growth and previous "group III-only" models of VLS growth are that (i) diffusion need not be considered while, on the contrary, (ii) evaporation must be taken into account (whereas at the self-catalyzed growth temperatures, the evaporation of Ga can safely be ignored, due to its low vapor pressure[47]).

We consider the various As currents I_i (numbers of atoms per unit time) to and from the droplet, corresponding to the four processes listed above. The current I_n corresponding to the transfer from liquid to stoichiometric solid is related to the NW growth rate $\rho_n = dL/dt$ (with L the NW length at time t, measured from a fixed reference) by $\pi R^2 \rho_n = \omega_p^S I_n$, where $\omega_p^S = a^3/4$ is the volume occupied by a III-V pair in ZB GaAs, with a the lattice parameter of the crystal. Since we want ultimately to compare the predictions of our model to measured growth rates, we similarly express all currents in terms of equivalent growth rates ρ_i:

$$\pi R^2 \rho_i = \omega_p^S I_i. \quad (1)$$

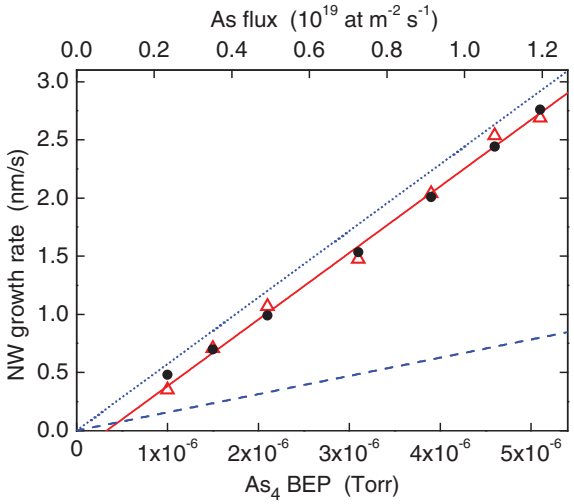

FIG. 2. (Color online) Growth rate of NW1 (up triangles), measured[15] as a function of As_4 BEP at $T_1 = 883$ K, and its linear approximation (full line). Dashed line: Growth rate equivalent to direct As flux impinging on droplet. Dotted line: Growth rate equivalent to direct flux plus minimum re-emitted flux. The circles are the best fit to the experimental data obtained using our model.

B. Feeding the droplet

We previously showed[49] that the direct atomic current ($i = d$), resulting from the interception by the droplet of the incident beam, writes $I_d = \kappa\,(\alpha,\beta)\,\pi R_d^2 J_d$. κ is generally a complicated function of the angles which however simplifies to $\kappa = 1$ when $\beta \geqslant \alpha + \pi/2$. Hence, using Eq. (1) and the geometric relations recalled in Appendix A 3 [Eq. (A10)], the contribution of the direct beam to the growth rate writes

$$\rho_d = \frac{\kappa\ \omega_p^S}{\sin^2\beta} J_d. \tag{2}$$

We assume here that all impinging molecules incorporate into the liquid droplet (unit accommodation coefficient), an hypothesis usually made in NW growth modeling.

In our previous work, we studied experimentally the growth rates of individual NWs and discussed the various As currents that feed the growth.[15] We concluded that the surface diffusion of adsorbed As species is negligible. However, the direct flux impinging on the droplet is insufficient to account for the growth rate (see also Sec. III A and Fig. 2). We attributed the missing current to a flux of As species re-emitted by the surfaces of the substrate (as previously proposed by Krogstrup *et al.*[11]) and of the neighboring NWs. It seems fair to assume that the corresponding contribution ($i = r$) to the growth rate is proportional to the direct contribution via a NW-dependent coefficient ϵ:

$$\rho_r = \epsilon \rho_d. \tag{3}$$

It is likely that ϵ depends on β but also on the distribution of NWs around the NW considered. Even for a given NW, ϵ might vary with time: As the NWs grow, the re-emitting sidewalls of the neighboring NWs extend, but at the same time shadowing effects[50] evolve; multiple reflections also probably intervene. This makes ϵ extremely difficult to calculate. Fortunately, it may be argued that, after the NWs have reached a sufficient length, ϵ should remain constant (due to shadowing, the substrate is no longer exposed to the direct beam), and the constant growth rate observed for individual NWs in our experiments strongly suggests that this is the case.[15] Anyway, this contribution is far from negligible: We estimated that ϵ was at least of the order of 2 for the NWs studied.[15] We will show that our model actually allows us to extract this coefficient from experiments for particular NWs.

C. Emptying the droplet: Evaporation and nucleation

The evaporation current ($i = e$) of a given atom or molecule is customarily assumed to be proportional to the equilibrium pressure of this species with the liquid. For arsenic, the most common species are As atoms and molecules As_n, $n = 2,3,4$. For bulk phases, the equilibrium pressure of each species, which is calculated in Appendix A 2, depends only on T and on the atomic concentration c_{As} in the liquid. At the typical self-catalyzed growth temperatures, the pressures of the various As species in equilibrium with a liquid, itself in equilibrium with solid GaAs, are very different from each other: The As_2 pressure is by far the largest one.[47] This remains true for the nonequilibrium concentrations c_{As} that we determine below. Considering this single As species, the evaporated atomic flux writes

$$J_e = k_e \frac{2\ p_2}{\sqrt{2\pi M k_B T}}. \tag{4}$$

Here the factor 2 stems from the fact that each As_2 molecule, of mass M, comprises two atoms, k_B is the Boltzmann constant, and $p_2\,(c_{As},T)$ the equilibrium pressure. Following Knudsen,[51] we have introduced an evaporation coefficient $k_e \leqslant 1$ to account for possible barriers hindering evaporation. The values of such evaporation coefficients remain largely unknown. The evaporated current is $I_e = S_d J_e$ and the equivalent growth rate is

$$\rho_e = J_e \frac{S_d \omega_p^S}{\pi R^2} = k_e \frac{1-\cos\beta}{\sin^2\beta} \frac{4\omega_p^S p_2}{\sqrt{2\pi M k_B T}}. \tag{5}$$

Finally, we turn to the formation of the NW itself. It is widely acknowledged that VLS growth of NWs of small enough radii proceeds ML by ML, via the formation of a single two-dimensional (2D) critical nucleus at the liquid-solid interface, followed by the rapid completion of the ML. This has been demonstrated for VLS growth catalyzed by foreign metals.[22,23,44,52–55] We assume that this is also the case for self-catalyzed growth although, to our knowledge, it remains to be verified. If, after nucleation, the complete ML forms in a time short compared to the mean time between nucleation events,[44,52–54] so that growth is mononuclear (one nucleation event per ML), the growth rate is set by the nucleation rate. Using the classical nucleation theory (CNT) for a solution of concentration c_{As}, the 2D rate of nucleation writes[56]

$$J_n = A(T)\ c_{As} \left(\frac{\Delta\mu}{k_B T}\right)^{1/2} \exp\left(-\frac{\Delta G_c}{k_B T}\right). \tag{6}$$

In Eq. (6), A is a prefactor which depends on temperature but neither on c_{As} nor on NW geometry, $\Delta\mu\,(c_{As},T)$ is the difference of chemical potential per III-V pair between the liquid of composition c_{As} and solid ZB GaAs, and ΔG_c is the nucleation barrier. $\Delta\mu$ is calculated in Appendix A 1 for bulk phases and the modification for a small droplet is given in Appendix A 3. The hypothesis underlying the presence of factor c_{As} in Eq. (6) is that attachment to subcritical nuclei is limited by As present in the liquid droplet and not by Ga, which is available there in abundance; however, this hypothesis is not crucial since the main dependence of J_n on c_{As} is via the nucleation barrier (see below). We consider, as usual in CNT, the formation of nuclei of fixed shape with linear dimension r, perimeter $\alpha_1 r$, and area $\alpha_2 r^2$ ($\alpha_1 = 2\pi$, $\alpha_2 = \pi$ for a disk of radius r; $\alpha_1 = 3$, $\alpha_2 = \sqrt{3}/4$ for an equilateral triangle of side r). If γ_e is the effective surface energy of the vertical edge of the 2D nucleus[23] (Fig. 1), the change of free energy of the system upon forming a nucleus of size r is $\Delta G = -\alpha_2 r^2 h\Delta\mu/\omega_p^S + \alpha_1 r h\gamma_e$. Minimizing ΔG gives the nucleation barrier

$$\Delta G_c = \chi\omega_p^S h\frac{\gamma_e^2}{\Delta\mu}, \tag{7}$$

with $\chi = \alpha_1^2/(4\alpha_2)$ ($\chi = \chi_d = \pi$ for disk-shaped nuclei and $\chi = \chi_t = 3\sqrt{3}$ for equilateral triangles). For ZB NWs growing along $\langle 111\rangle$, $h = a/\sqrt{3}$, and $\omega_p^S h = a^4/(4\sqrt{3})$.

The formation of the ZB structure in self-catalyzed growth suggests that nucleation occurs not (or not only) at the triple phase line[23] but anywhere else on the top facet of the NW.[10] Then, the probability of forming a critical nucleus, per unit time, is $\pi R^2 J_n$. Since we suppose that nucleation is quickly followed by the completion of the full ML, the corresponding current is $I_n = h(\pi R^2)^2 J_n/\omega_p^S$ and the equivalent growth rate is

$$\rho_n = \pi R^2 h J_n. \tag{8}$$

In all calculations we account for the effect of the small size of the droplet on p_2 and $\Delta\mu$ (Appendix A 3), but this hardly modifies the results. On the other hand, we ignore the variations of group V concentration induced by the fast stages of nucleation and growth of new MLs that suddenly deplete the droplet and are separated by long refill periods. We showed that this effect leads to sub-Poissonian nucleation statistics (anticorrelation of nucleation events).[44] However, it generally affects little the average growth rate. Namely, based on our simulations of Au-catalyzed growth[44] (we have not yet studied self-catalyzed growth in this respect), the growth rate calculated in the sub-Poissonian regime by averaging over a sequence of simulated nucleation events is close to the constant (Poissonian) growth rate calculated for a fixed droplet composition equal to the average composition observed in the simulations of the sub-Poissonian case (provided of course that we use the same model parameters for the nucleation rate). Thus, we do not describe the short term fluctuations of the nucleation rate, and ρ_n and c_{As} should be understood as values averaged over several nucleation cycles. This is consistent with fitting our model to experiments which average the growth rate over many such cycles.[15]

III. MODELING EXPERIMENTS AND EXTRACTING MODEL PARAMETERS

Our aim in Secs. III and IV is fourfold. We first demonstrate that our model can fit accurately the NW growth rates measured in a series of experiments where either the As beam pressure or the temperature are varied systematically (Sec. III B). By optimizing these fits, we extract precise values of the few unknown parameters that specify the model (Sec. III C). We then show that values of quantities pertaining to the growth of individual NWs but so far inaccessible to experiment can be straightforwardly obtained by applying our model (Sec. III D). Finally, in Sec. IV we show that our model predicts the growth rate of any self-catalyzed GaAs NW of known geometry, in given growth conditions.

A. Method and general considerations

We want to find the best values of the parameters γ_e and $A\,(T)$ that specify the nucleation rate in our model by fitting this model to series of measurements of the growth rate of single NWs of known geometry in precisely determined growth conditions, taken from our previous work[15] (where $\alpha = 35^\circ$). We suppose known the values of several secondary parameters. Namely, we take $\chi = \chi_t$, $k_e = 1$ and assume perfect accommodation of the As gaseous species by the droplet (see above). These choices are discussed in Sec. V A.

Then, from Eqs. (6)–(8), the nucleation-mediated growth rate of a NW of known radius is fixed by the two *model parameters* γ_e and $A\,(T)$, which depend only on the material system considered. In addition, the nucleation rate also depends on the difference of chemical potential $\Delta\mu$, which itself depends on temperature and As concentration c_{As} in the liquid (see Appendix A 1). This concentration, which must change with growth conditions and is also likely to be different for each NW in given conditions, is unknown. Hence, the problem cannot be solved by the sole consideration of nucleation since the number of experimental data points (growth rate in given growth conditions) is always less than the number of unknowns (model parameters plus one As concentration per data point).

However, c_{As} may be determined for each data point of a given series by assuming material balance, i.e., that the currents adding atoms to the droplet exactly compensate for those that deplete it (in doing so, we do not restrict ourselves to stationary growth; we simply average the short-term fluctuations of the As concentration due to random nucleation and ML growth mentioned above[44]). This will be shown in Sec. III B. There we will first model the data of Fig. 2, which consist of measurements of the growth rate of a single NW (NW1) at temperature $T_1 = 883$K, as a function of the incident As flux,[15] expressed as a measured As_4 beam equivalent pressure (BEP) p_{As_4} (lower scale). We previously determined[15] the conversion factor between BEP and actual atomic flux J_d (valid for our MBE setup) to be $\eta = J_d/p_{As_4} = 2.3\times10^{24}$ atom m^{-2} s^{-1} Torr^{-1} (see upper scale).

This pressure series displays features which have become familiar for self-catalyzed GaAs growth.[6,15] Before modeling it, we briefly discuss these features and their implications

for our model. First, the growth rate increases quasilinearly with incident flux. From Eqs. (6)–(8) and from the calculation of $\Delta\mu$ (Appendix A 1, Fig. 10), any increase of the growth rate *at fixed T and for a NW of given radius* implies an increase of c_{As}. However, since the nucleation rate depends in an *a priori* strongly nonlinear fashion on As concentration, the observed quasilinearity suggests that c_{As} and $\Delta\mu$ do not vary much over the entire experimental range. Second, the linearly extrapolated growth rate (full line in Fig. 2) cancels at a nonzero pressure. This was rightly interpreted as related to the As vapor pressure at the droplet surface.[6] In the terms of our model, there is a minimal BEP for which c_{As} is such that the evaporated current [Eq. (5)] just balances the sum of the direct current [Eq. (2), dashed line in Fig. 2] and re-emitted current [Eq. (3)]; however, this flux is not equal to the zero growth rate linear extrapolation since the growth rate is nonlinear at low As flux (see Sec. IV B). Third, since the sum of the direct and re-emitted currents scales as $(1+\epsilon)J_d$, the nonzero intercept implies that there is a minimum value ϵ_m of ϵ, given by the slope of the line passing by the origin and parallel to the quasilinear experimental curve (dots in Fig. 2). For this particular ϵ (about 2.6 for the present data), the evaporation equivalent growth rate, read as the vertical distance between the full and dotted lines, would be the same for all incident fluxes. This cannot however be the case, since the increase of growth rate with BEP (at fixed R and T) has to be induced by an increased c_{As}, which itself enhances evaporation (Appendix A 2, Fig. 10), so that the available current (direct + re-emitted) actually has to increase faster than the experimental growth rate; this corresponds to $\epsilon > \epsilon_m$.

B. Modeling experimental growth series

We first model the pressure series of Fig. 2. NW1 has radius $R \approx 32$ nm and the droplet contact angle is $\beta_1 \approx 125^\circ$, hence $\kappa = 1$ (Sec. II B). Material balance dictates that the measured growth rate ρ_m equals the algebraic sum of the direct, re-emitted, and evaporated contributions, calculated respectively from Eqs. (2), (3), and (5): $\rho_m = \rho_d + \rho_r - \rho_e$. This is obviously independent of the hypothesis that growth occurs via nucleation. Rates ρ_d, ρ_r, and ρ_e depend on NW geometry, which is supposed to be known. Actually, the NW radius R is precisely measured in our transmission electron microscopy (TEM) images. The contact angle β is also measured precisely but the post-growth value might differ from the value during growth. In Sec. V A we evaluate the effect on our results of a plausible error on β.

In the material balance equation, only ρ_e depends on c_{As} [Eqs. (5), (A8), and (A9)], whereas ρ_d depends only on the known direct As flux [Eq. (2)]. In addition, the re-emitted contribution ρ_r depends on unknown and NW-specific parameter ϵ (which nevertheless, as discussed above, is not expected to change with growth conditions). The equation thus involves two NW-related unknowns, ϵ and c_{As}. Hence, if one fixes an arbitrary value of ϵ for the whole series, one can deduce the As concentration $c_{\mathrm{As},q}$ from the measured growth rate $\rho_{m,q}$ for each data point q ($q = 1, \ldots, Q$, $Q = 7$), using solely material balance. Introducing the extra unknown ϵ effectively eliminates all unknown concentrations and makes the problem tractable. In practice, for each ϵ arbitrarily chosen

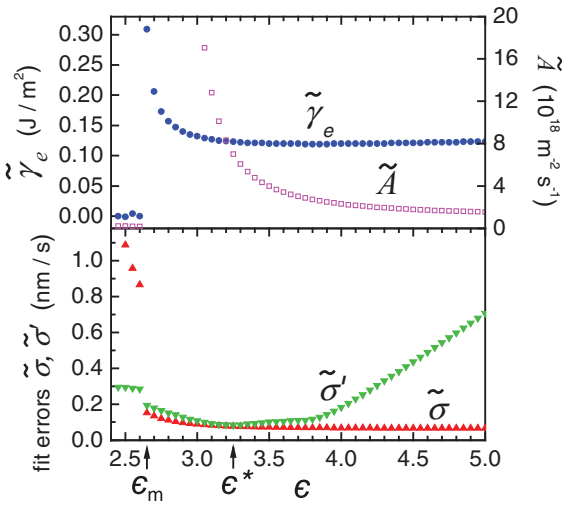

FIG. 3. (Color online) Bottom: Variations with test value of re-emission constant ϵ, of the normalized errors $\tilde{\sigma}$ and $\tilde{\sigma}'$ (up and down triangles) for the fits of NW1 and NW2, respectively. Top: Variation with ϵ of the optimal values of nucleus edge energy γ_e (disks) and prefactor $A(T_1)$ (empty squares). The fits made with $\epsilon \leqslant \epsilon_m$ lead to large errors and unphysical values of γ_e and $A(T_1)$.

in a wide range of values, we get the set of concentrations $c_{\mathrm{As},q}$. We then calculate the normalized error $\sigma(\epsilon, A, \gamma_e) = [Q^{-1}\sum_{q=1}^{Q}\{\rho_{m,q} - \rho_{n,q}(\epsilon, A, \gamma_e)\}^2]^{1/2}$, where $\rho_{n,q}$ is the nucleation-mediated growth rate calculated using model parameters $A(T_1)$ and γ_e and concentration $c_{\mathrm{As},q}$ [Eqs. (6)–(8)]. Figure 3 (bottom) gives the variation with ϵ of the minimum $\tilde{\sigma}(\epsilon)$ of σ, taken over all values of model parameters $A(T_1)$ and γ_e. We call $\tilde{A}(T_1, \epsilon)$ and $\tilde{\gamma}_e(\epsilon)$ the values which realize this minimum. Clearly, although we can safely exclude values of ϵ less that about 2.65 (for which the error is very large and γ_e takes unphysically low or even negative values, thereby confirming the minimum value of ϵ discussed in Sec. III A), our test does not discriminate among a wide range of values and does not even exclude unreasonably large values. Hence, the best model parameters cannot be determined at this stage.

Fortunately we can lift this indetermination by combining the previous results with the analysis of series of growth rate measurements on single NWs, at fixed incident flux but variable temperature. We use the data[15] for NW2, obtained under $p_{\mathrm{As}_4} = 4.8 \times 10^{-6}$ Torr (Fig. 4). For this NW, $R \approx 37$ nm and $\beta = \beta_2 \approx 125^\circ$. We use the information gained in modeling the pressure series to calculate the nucleation-induced growth rate for this series. Namely, in Eqs. (6) and (7) we restrict ourselves to the best couples of model parameters $\tilde{A}(T_1, \epsilon)$ and $\tilde{\gamma}_e(\epsilon)$ determined previously, each associated to an arbitrary value of ϵ (not being a basic model parameter, ϵ is not of primary interest; it is merely used as an index for this particular couple of parameters). However, we must now account for the variation of prefactor A [Eq. (6)] with temperature. Following CNT for 2D nucleation,[56] we write $A(T) = A' \exp[-E_a/(k_B T)]$, where A' is a temperature-independent parameter and E_a is an energy barrier for the transfer of an As atom from the liquid phase to the edge of the nucleus. E_a is *a priori* unknown; however, since the prefactors

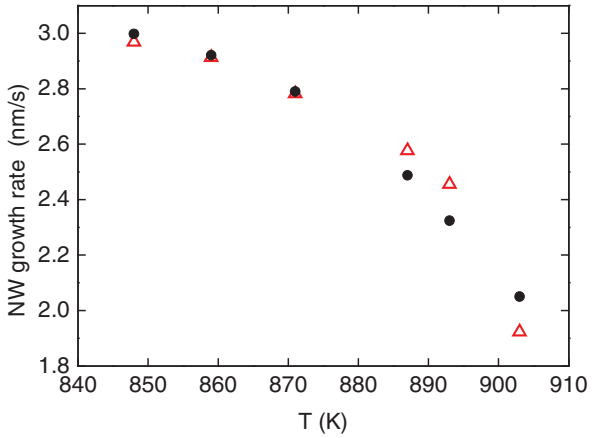

FIG. 4. (Color online) Growth rate of NW2 measured as a function of growth temperature (triangles). The disks give the differences between the growth rates equivalent to total incoming (direct + re-emitted) and evaporated currents corresponding to the best fit by our model (see text).

in the nucleation rate must match for $T = T_1$, the choice of E_a fixes that of A', according to $A' \exp[-E_a/(k_B T_1)] = \tilde{A}(T_1,\epsilon)$.

Now, for each arbitrary couple of values of ϵ [i.e., $\tilde{A}(T_1,\epsilon)$, $\tilde{\gamma_e}(\epsilon)$] and E_a, we first find the As concentration $c_{\mathrm{As},q}$ for each data point q ($q = 1,\ldots,Q'$, $Q' = 6$) of the temperature series by equating the measured growth rate $\rho'_{m,q}$ to the nucleation-induced growth rate $\rho'_{n,q}$ calculated for $c_{\mathrm{As},q}$. Since p_2 is a known function of c_{As} and T (Appendix A 2), this concentration also produces a certain evaporation rate $\rho'_{e,q}$ [Eq. (5)]. We now invoke As material balance. Namely, we first choose arbitrarily the unknown re-emission constant ϵ' pertaining to NW2 and calculate the normalized error $\sigma'(\epsilon,\epsilon',E_a) = [Q'^{-1}\sum_{q=1}^{Q'}\{(1+\epsilon')\rho'_d - \rho'_{e,q} - \rho'_{n,q}\}^2]^{1/2}$, with ρ'_d the direct growth rate, which is fixed for this series. We then minimize σ' over all values of E_a and ϵ' to obtain the quantity $\tilde{\sigma}'(\epsilon)$, shown in Fig. 3. The variations of $\tilde{\sigma}'$ with ϵ are much more pronounced than those of $\tilde{\sigma}$. In particular, $\tilde{\sigma}'$ shows a marked minimum around $\epsilon^\star \approx 3.25$, a value only slightly larger than ϵ_m (this minimum is realized for $\epsilon' = 3.15$ and $E_a = 0$; see below). Around $\epsilon^\star$, the normalized errors are less than 0.1 nm/s for both pressure and temperature series. Again, the value of $\epsilon^\star$ (*a priori* valid only for NW1) is of less interest than those of the associated model parameters $\tilde{A}(T_1,\epsilon^\star)$ and $\tilde{\gamma_e}(\epsilon^\star)$, to be given in the next section. The quality of the fits is illustrated in Figs. 2 and 4 for the pressure and temperature series, respectively.

C. Recommended values of the model parameters

We have just determined $\epsilon^\star$ as the best value of the re-emission constant for NW1 and consequently $\tilde{A}(T_1,\epsilon^\star)$ and $\tilde{\gamma_e}(\epsilon^\star)$ as the best values of the model parameters A (at temperature T_1) and γ_e. The analysis of the temperature series involves an additional optimization over parameter E_a. Although the quality of the fit is rather insensitive to the value of E_a (we explored the range from 0 to 1 eV), smaller values consistently give marginally better fits (at least for the preferred ϵ). We thus take $E_a = 0$; then, $A(T) = A'$ is independent of temperature and must be taken equal to $\tilde{A}(T_1,\epsilon^\star)$. In the following, we fix the model parameters to their best values and simply note them γ_e and A. These best values are

$$\gamma_e = 0.123\ \mathrm{J\,m^{-2}}, \quad A = 7.01 \times 10^{18}\ \mathrm{m^{-2}\,s^{-1}}. \tag{9}$$

Using these values in Eqs. (6)–(8) (with A independent of T) gives the nucleation rate in units of $\mathrm{m^{-2}\,s^{-1}}$. Recall that, in Eq. (6), c_{As} ($\sim$1%) is the atomic concentration and that, in Eqs. (6) and (7), $\Delta\mu(c_{\mathrm{As}},T)$ is calculated per III-V pair (see Appendixes A 1 and A 3).

D. Evaluating experimentally inaccessible quantities for individual NWs

From the preceding analysis, we can also obtain extra information pertaining to actual growth experiments. Indeed, for both pressure and temperature series, the procedure of Sec. III B involves the determination of c_{As} for each set of growth conditions (As flux, temperature). Because it is extremely low, this concentration seems inaccessible to experiment and has indeed never been measured. Our determination of c_{As} is thus very welcome, all the more so that several thermodynamic quantities of key importance in the theory of NW growth, and so far at best roughly estimated, are readily calculated from c_{As}, in particular the difference of chemical potential $\Delta\mu(c_{\mathrm{As}},T)$ between liquid and solid ZB GaAs (Appendix A 1) and the nucleation barrier ΔG_c [Eq. (7)] (note for instance that for Au-catalyzed growth the estimates of $\Delta\mu$ span a range extending from a few meV or tens of meV[22,27,57] to several hundreds of meV[23,31,43,44] per pair). These quantities are plotted in Fig. 5 for each data point of the experimental series analyzed in Sec. III B.

As for the pressure series [Fig. 5(a)], the As concentration increases with the direct As flux. This was expected since, at constant NW radius and fixed temperature, according to Eqs. (6)–(8), the observed increase of the growth rate must be due to an increase of $\Delta\mu$, which itself can only be due to an increase of c_{As} (Appendix A 1 and Fig. 10). As forecast in Sec. III A, c_{As} is not far from varying linearly with the As_4 BEP, although a slightly negative curvature can clearly be seen. c_{As} is of the order of 10^{-2} but varies by more than 50% over our pressure range. This gives differences of chemical potential increasing between about 115 and 150 meV/pair.

The results for the temperature series [Fig. 5(b)] are far less intuitive. We predict that, despite the observed decrease of the growth rate, the As concentration in the droplet should *increase* with temperature. However, Fig. 5(b) shows that this increase of c_{As} does not induce an increase of $\Delta\mu$ with T. $\Delta\mu$ actually decreases, due to the dominating effect of temperature (Appendix A 1 and Fig. 10), which correctly induces a decrease of the growth rate. At the same time, the increases of c_{As} and T concur to enhance evaporation. For more details, see Sec. IV B.

IV. PREDICTIVE MODELING

In this section we show how, using the model parameters determined in Sec. III, we can predict the growth rate of any NW of given geometry in given growth conditions. Our predictions stand the test of all comparisons with our experimental data (including those not used in the determination of the model

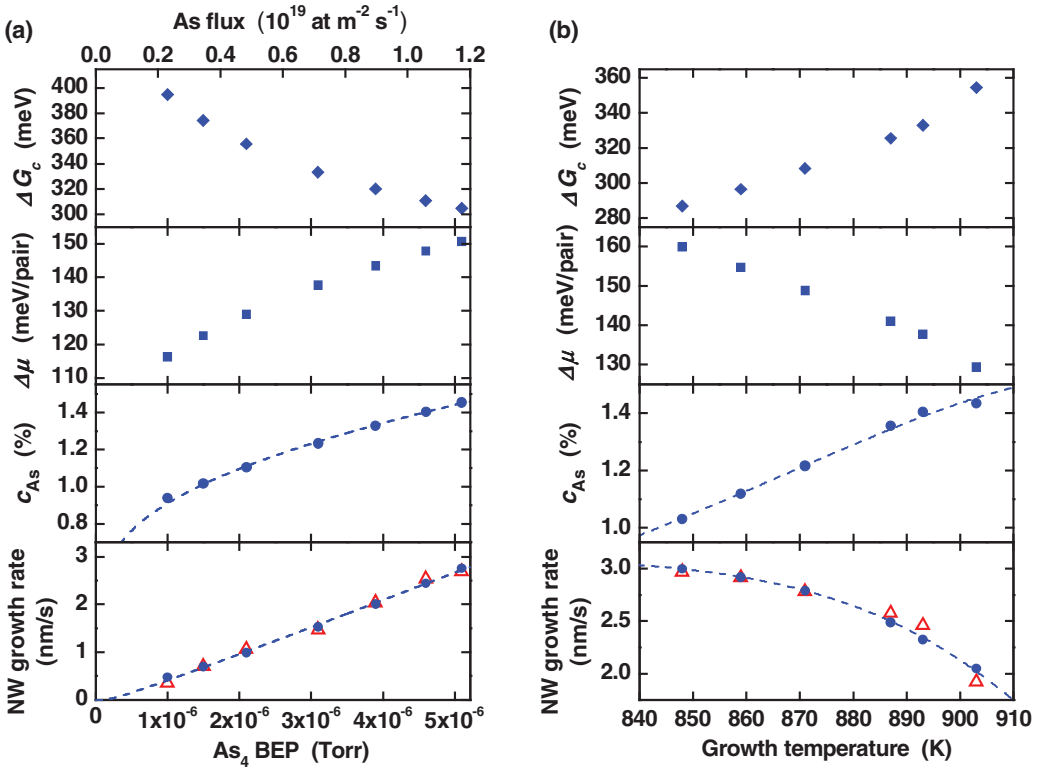

FIG. 5. (Color online) (a) Bottom panel: Growth rates measured (triangles) and calculated (disks) for NW1, as a function of incoming As flux, at temperature $T_1 = 883$ K (as in Fig. 2). Three upper panels: As concentration in the droplet, difference of chemical potential between liquid of composition c_{As} and solid ZB GaAs, and nucleation barrier, calculated for each discrete data point of bottom panel. In the two bottom panels, the dashed lines are calculations extended to the whole pressure range, made for NW1 using the best model parameters (Sec. III C) and the method of Sec. IV. The As flux is expressed as BEP (lower scale) and as absolute atomic flux, using the value of η given in text (upper scale). (b) Same as (a) for NW2, as a function of growth temperature.

parameters). In addition, we predict the behavior of the NW growth rate and related quantities in growth conditions as yet unexplored.

A. Method

Let us consider a NW of given geometry (radius R, droplet contact angle β) in given growth conditions, in particular temperature T and As_4 flux. Since the model parameters γ_e and $A(T)$ are now fixed (Sec. III C), the nucleation-induced growth rate ρ_n of this NW depends only on the As concentration in the droplet [Eqs. (6)–(8)]. As in the experimental case, c_{As} is *a priori* unknown, but it may be determined by invoking once again As material balance, which prescribes that

$$(1+\epsilon)\,\rho_d = \rho_e\,(c_{As},T) + \rho_n\,(c_{As},T)\,. \qquad (10)$$

This equation features the re-emission constant ϵ pertaining to the modeled NW. Since ϵ accounts for As re-emitted by substrate and neighboring NWs, a NW cannot in general be modeled in isolation. Instead, we must picture it as part of an ensemble of many NWs. Two types of such samples are conceivable. Either the NWs are fairly closely packed and distributed more or less randomly; then, ϵ is likely to vary with the environment of the NW considered. Simulating such an assembly of NWs and modeling their growth goes beyond the scope of the present work, and calculating the re-emission seems very difficult. The simplest is thus to count ϵ as an additional (unknown) growth parameter. On the other hand, we may imagine two categories of samples where the re-emission coefficient could possibly be calculated: low density samples where a given NW would be exposed to re-emission only from the substrate, or else periodic arrays of NWs. For all categories of samples, it might also be possible to determine ϵ experimentally and use its value as an input parameter. For random samples, this would have to be done as a function of NW density, without however accounting for local fluctuations. Such density fluctuations would not occur for regular arrays or isolated NWs. In the future, ϵ might thus become a known quantity but, despite some preliminary calculations,[58] this is far from being achieved. We thus consider ϵ as an input parameter (an extra growth condition) depending on the NW considered. However, our experiments and modeling indicate that ϵ might not vary much even in random samples.

Then, using Eq. (2), the left side of Eq. (10) is known for any given direct As flux. Since the right side of Eq. (10) depends only on input temperature T and As concentration c_{As}, the latter can be uniquely calculated for any given set of growth conditions (As flux, T, ϵ). The growth rate is then straightforwardly obtained via Eqs. (6)–(8) using the values of the model parameters supplied in Sec. III C. As in the experimental case (Sec. III D), all thermodynamic quantities of interest can then be calculated from c_{As}.

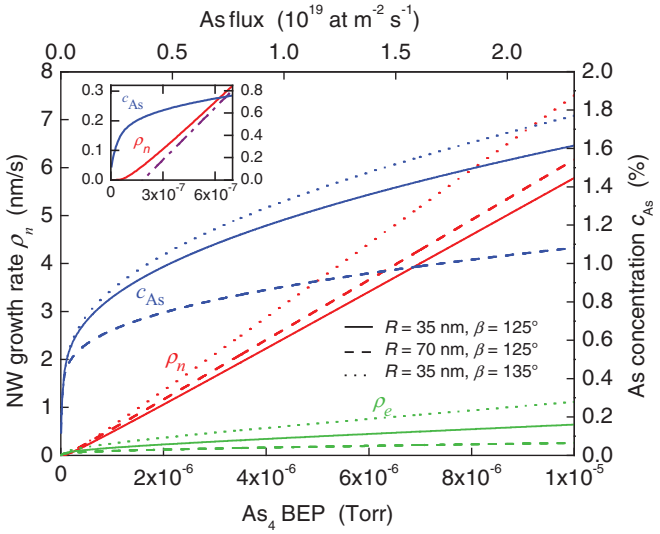

FIG. 6. (Color online) NW growth rate ρ_n (red lines, left scale), equivalent evaporation rate ρ_e (green lines, same scale), and As concentration in the droplet (blue lines, right scale) calculated using our model as a function of the incident As flux for three simulated NWs having the different geometries (NW radius, droplet contact angle) indicated. Other parameters: $\epsilon = 3.1$, $T = 873$ K. The As flux is expressed as absolute atomic beam flux (upper scale) and as BEP, using value of η given in text (lower scale). The inset details the variations of the growth rate and As concentration at low fluxes (units as in main panel) for the NW with $R = 35$ nm and $\beta = 125°$; the dash-dotted line is the linear approximation of the NW growth rate at high As flux.

B. Modeling NW growth as a function of As flux, NW radius, and temperature

This method is illustrated in Fig. 6 for a simulated pressure series. We model three arbitrary NWs with different geometries. Doubling the NW radius from 35 to 70 nm leads to only a very modest increase of the growth rate. As detailed below, this is in agreement with our experiments.[15] The droplet contact angle has a larger effect on the growth rate. Our model allows us to explore growth under As fluxes both larger and smaller than those hitherto studied experimentally.[15] At high fluxes, the growth rate and c_{As} still vary quasilinearly with As flux. When the flux is decreased, c_{As} deviates markedly from linearity before the NW growth rate. However, at very low As fluxes (Fig. 6, inset), the NW growth rate is also strongly nonlinear. As a consequence, NWs might still grow under As fluxes lower than predicted by the linear extrapolation of the high-temperature data.[6]

The variations of the growth rate with NW radius are further explored in Fig. 7. At $T = 883$ K, we find only a small variation of the NW growth rate in a large range of NW radii. Between radii of 25 and 40 nm, the growth rate increases by only 14%. This compares closely with our experiments where, over the same range and at the same temperature, an increase of about 10% of the total NW length was measured.[15] However, we predict a sharp drop of the growth rate at smaller NW radii. At higher temperature (Fig. 7, triangles), the growth rate should vary faster with NW radius (unless this radius is very small).

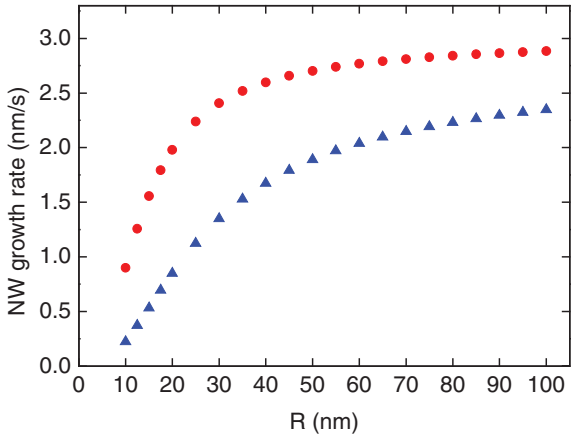

FIG. 7. (Color online) Calculated variation of the NW growth rate as a function of NW radius under given As flux ($J_d = 1.1 \times 10^{19}$atom m^{-2} s^{-1}, corresponding to 4.8×10^{-6}Torr As$_4$ BEP with η given in text) at $T = 883$ K (disks) and 913 K (triangles). $\beta = 125°$, $\epsilon = 3.1$.

These variations of the growth rate with NW radius can be clarified by modeling a temperature series. Figure 8 shows the variations with temperature of the growth rate ρ_n, equivalent evaporation rate ρ_e, and As concentration in the droplet, calculated for four NWs (including those of Fig. 6). Here again we explore a range of the relevant growth parameter (T) wider than in our experiments. Let us first focus on the two NWs with $\beta = 125°$ and radii of 35 and 70 nm, respectively. At low T, their growth rates are equal. Since evaporation is then negligible (see ρ_e curves), As material balance [Eq. (10)] implies that the total incoming current $I_d + I_r$ equals the nucleation current I_n. However, the former scales as S_d and hence R^2 [Eqs. (1) and (2)], whereas the latter, as explained in Sec. II C, scales as $R^4 J_n$. Hence, material balance can only be guaranteed if the nucleation rate J_n is *less* for the wider NW than for the narrower one (namely, 4 times smaller for the present radii). This in turn implies *smaller* values of $\Delta\mu$ and hence c_{As} for the wider NW at given T (as already seen

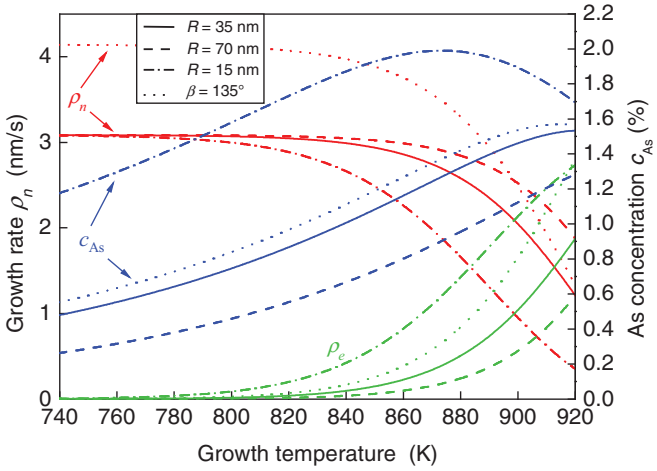

FIG. 8. (Color online) Same as Fig. 6 as a function of growth temperature for four simulated NWs. $\beta = 125°$ for the three NWs labeled by their radius R, and $R = 35$ nm for the NW labeled by β. ϵ and direct As flux as in Fig. 7.

in Fig. 6). At higher temperature, As evaporation becomes significant and the growth rates of both NWs start to decrease. However, since evaporation increases with c_{As} (Appendix A 2 and Fig. 10), the growth rate of the narrow NW (with higher c_{As}) decreases faster than that of the wide one, to the effect that the latter now grows faster than the former. Examination of the NW with $R = 15$ nm confirms this explanation (Fig. 8). At very low T, its growth rate is the same as that of the former two and hence its c_{As} is even higher, so that evaporation comes into play at even lower temperatures.

To summarize, we predict that, if the radius is not too small, the growth rate is quasi-independent of radius at low growth temperature and increases with radius at higher temperatures. The narrow range of growth rates observed in our experiments[15] is reproduced by our model (Fig. 7, disks). It results from the fact that our growth temperature ($T = 883$ K) is moderate and that we did not synthesize very narrow NWs. We predict an even narrower range of growth rates at low growth temperature and a wider range either at higher growth temperature or if narrower NWs became available.

This modeling of temperature series clarifies our observation of an increase of c_{As} with T at given NW radius [Sec. III D, Fig. 5(b)]. Actually, for each NW, as T increases, c_{As} reaches a maximum and then decreases (Fig. 8). Again, at low T, evaporation being negligible, nucleation alone must balance the fixed sum of the direct and re-emitted currents. When T increases in this domain, $\Delta\mu$ would decrease if c_{As} were fixed (Appendix A 1 and Fig. 10), so that c_{As} must actually increase to maintain the nucleation rate. However, at higher temperature, evaporation becomes effective and increases sharply with T and c_{As}, faster than nucleation decreases. c_{As} must then decrease to preserve As balance.

V. DISCUSSION AND CONCLUSIONS

A. Impact of imperfectly known quantities on the values of the model parameters

To determine the basic parameters of our model, we made use of the experimental growth rates of only two NWs. It would be desirable to confirm these values by fitting the growth rates of other NWs, but this has not been done yet, mainly because the necessary TEM analysis[15] is very time consuming. However, we analyzed another NW belonging to the same pressure series as NW1 and found very similar growth rates (which implies that, although it had a different environment during growth, its re-emission constant was very close to that of NW1). Let us first discuss briefly the possible sources of error in the measurements, which were described in detail by Ramdani *et al.*[15] Since the model parameters were extracted from a joint fit of a full pressure series and a full temperature series, we believe that random errors on the measurements of growth rate, As_4 pressure, or temperature somehow compensate each other, although this is difficult to quantify. We estimate that the length grown in the fixed time intervals between markers[15] may be determined to within ± 1 ML, so that the error on the measured growth rates is at most of a few percent. As regards the control parameters (T and As flux), the ratios of the As_4 BEPs for a given pressure series are also known to within a few percent. Similarly, the differences between two temperatures of a given series are probably very small, but the absolute temperature are not known to better than about 10 K. Our determination of the model parameters is thus likely to be affected mainly by possible systematic errors on As_4 BEP and growth temperature. In addition to As flux and sample temperature, when we fitted the experimental data, we assumed that several secondary parameters on the one hand, the geometry of the NWs on the other, were known. We now discuss the implications of an imperfect knowledge of all these quantities on our results.

Over and above the model parameters γ_e, A, and E_a that were optimized, there are three NW-independent quantities that appear in our equations, namely χ [Eq. (7) for nucleation barrier], η [relating direct current appearing in Eq. (2) to measured As_4 BEP], and k_e [Eq. (4) for evaporation]. We also assumed that the liquid accommodates the impinging As molecules (directly or after re-emission) with unit probability. We shall consider these quantities in turn. Equation (7) readily shows that our fitting procedure actually determines the product $\chi\gamma_e^2$; the value of γ_e obtained assuming $\chi = \chi_t$ can thus straightforwardly be adapted to nontriangular nucleus shapes (for instance, we find $\gamma_e = 0.158$ J m^{-2} for disk-shape nuclei). Ratio η was painstakingly measured in our previous work.[15] However, it is clear that only the total current into the droplet $I_d + I_r = (1+\epsilon)\kappa\pi R_d^2 J_d$ intervenes in the fitting procedure. Hence, any modification of η affecting J_d will be compensated by a change of ϵ. The same holds for an accommodation coefficient less than 1. Therefore, only the re-emission coefficient will be altered by an error on η or on the accommodation coefficient, not the model parameters. On the other hand, changing the value of k_e affects the values of the model parameters, because the use of the known dependence of evaporation on c_{As} (Appendix A 2) is crucial in our procedure (see below).

Several parameters specific to the particular NWs used in the determination of the model parameters (Sec. III B) are also imperfectly know. Any variation of these NW-specific parameters affects the values of the model parameters given in Sec. III C. In particular, whereas the NW radii can be measured with great accuracy, the values of the contact angles β_1 and β_2 for NWs 1 and 2 during growth could be different from, and probably larger than, those that we measure after growth (note for instance that the post-growth angles measured by Kim *et al.* are even lower[59]). The temperatures measured during the experiments are also imperfectly known. We decided against considering these NW-specific quantities as unknown and finding their best values by optimizing our fits. This is somehow validated by the excellent fits that we obtain by optimizing only the three basic model parameters. However, we may evaluate the effects of uncertainties on these neglected parameters. To this end, we assume for one of them a value different from the value retained in Sec. III B, keeping the others at their previous values. We then carry out the procedure detailed in Sec. III B and end up with a new pair of model parameters (γ_e, A) (in all cases, we find an optimal value $E_a = 0$). The results are summarized in Table I.

Let us first discuss the effect of uncertainties affecting experimental geometry (sets 2 and 3 in Table I) or growth temperature (sets 4 and 5). Upon the changes assumed in these sets, the nucleus edge energy γ_e varies by about $\pm 15\%$

TABLE I. Modeling the growth of NW1 and NW2 using different values of NW-specific parameters or evaporation coefficient. Reference set (1): All geometrical parameters and growth conditions as in Sec. III. For sets 2 to 4, one of the parameters (for either NW1 or NW2) is changed to the value indicated in the second column. For set 5, all growth temperatures of the temperature series are shifted down by 10 K. For sets 1 to 5, $k_e = 1$. For set 6, $k_e = 0.5$ and NW geometrical parameters and growth conditions as in set 1. For each set, γ_e and A are the values of the model parameters found from the best fits to the experimental data of Figs. 2 and 4, $\tilde{\sigma}$ and $\tilde{\sigma}'$ are the fit errors for the pressure and temperature series (as in Sec. III B), and c_m and c_M are the values of c_{As} for the minimum and maximum As_4 BEPs of the pressure series (NW1, see Fig. 2).

Set	Parameter change	γ_e (J m^{-2})	A (10^{18} m^{-2} s^{-1})	$\tilde{\sigma}$ (nm/s)	$\tilde{\sigma}'$ (nm/s)	c_m (%)	c_M (%)
1	None	0.123	7.01	0.077	0.084	0.94	1.45
2	$\beta_1 = 135°$	0.108	2.34	0.064	0.094	0.90	1.54
3	$\beta_2 = 120°$	0.123	7.01	0.077	0.102	0.94	1.45
4	$T_1 = 893$ K	0.103	1.73	0.067	0.097	0.96	1.66
5	$\delta T_2 = -10$ K	0.142	12.8	0.079	0.084	1.07	1.65
6	$k_e = 0.5$	0.149	12.5	0.079	0.087	1.31	2.01

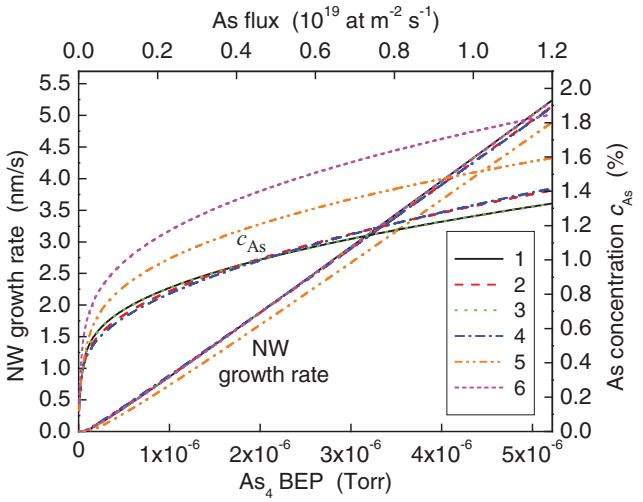

FIG. 9. (Color online) Calculation of the growth rate of a given NW and of the As concentration in the droplet as a function of incident As flux, using various pairs of model parameters (γ_e, A) (given for sets 1 to 6 in Table I). NW geometry: $R = 45$ nm, $\beta = 140°$. Growth conditions: $T = 873$ K, $\epsilon = 3.5$. Double horizontal scale as in Fig. 6.

around the value given in Sec. III C. γ_e, which appears in the exponential term of the nucleation rate, has a large effect on the latter. Since we fit the same data as before, even such moderate changes in γ_e are compensated by large changes of the other model parameter (prefactor A) together with modest changes of c_{As} at each data point. This does not compromise the validity of our model. Indeed, the quality of the fits (given by $\tilde{\sigma}$ and $\tilde{\sigma}'$ in Table I) remains nearly as good as for the reference set. The predictive character of the model is also preserved. To prove this, we use each of these alternative sets of model parameters (γ_e, A) to simulate the growth (under a range of As fluxes) of an arbitrary NW differing markedly in terms of geometry ($R = 45$ nm, $\beta = 140°$) and growth conditions ($T = 873$ K, $\epsilon = 3.5$) from NW1. Figure 9 shows that the net effect on the NW growth rate is less than 7% over the whole As_4 BEP range considered. The effect on c_{As} is also very small, except for the change in T_2. Note that the changes assumed for the NW-specific parameters are of the order of the estimated uncertainties and that changes either larger or with the opposite sign (i.e., $\beta_2 = 135°$) soon lead to considerably worse fits. Finally, even the huge change of evaporation coefficient that we assumed (set 6) has an effect of the same order on the model parameters and little effect on the growth rate (Fig. 9).

B. Summary and conclusions

In summary, we have developed a quantitative and predictive model for the self-catalyzed VLS growth of GaAs NWs. The model is based on the sole consideration of the As species and describes all the mechanisms of exchange of As between the vapor, liquid, and solid phases that we believe relevant, namely direct impingement of molecules on the droplet, their re-emission by the neighboring surfaces, evaporation from the droplet, and nucleation of GaAs at the solid-liquid interface.

The model reproduces quantitatively our measurements of the NW growth rate as a function of As_4 flux, growth temperature, and NW radius.[15] The values of the two main model parameters, namely the nucleus edge energy and the prefactor appearing in the nucleation rate [Eq. (6)], have been determined by fitting these data. The growth rate of a NW of known geometry under given As flux and at given temperature can then be calculated, provided the fraction of the As flux that is re-emitted by its environment is known. The model provides not only the growth rate but also the As concentration in the droplet and all quantities that depend on it (chemical potential, nucleation barrier, evaporation rate, ...). We find that in typical growth conditions, this concentration is of the order of 1%, as has been proposed for VLS growth (whatever the growth method and catalyst) on the basis of other experiments and calculations.[11,23,31,33,44,45] Measuring such low concentrations, especially during growth, seems beyond the reach of current analysis techniques.

Our model reproduces well-documented effects (such as the quasilinear variation of the growth rate with As flux at moderate and high fluxes) but also predicts many effects that have not been observed or forecast so far. Among these are the nonlinear variation of the growth rate with low As fluxes, the temperature-dependent variation of the growth rate with NW radius, the variation of the As concentration in the droplet with As flux, temperature, and NW radius.

To our knowledge, this is the first model of NW growth based on a small number of model parameters that are all assigned values validated by experiments. The all-important effective nucleus edge energy γ_e (which reduces to the energy of the interface between nucleus edge and liquid, if nucleation occurs away from the triple phase line, as assumed here on the basis of the observation of pure ZB) has not been determined before, although estimates ranging from a few tenths to about 1 J m^{-2} have been proposed for Au-catalyzed growth.[23,31] Assuming triangular nuclei, we find a value of 0.123 ± 0.2 J m^{-2}. This range allows for reasonable uncertainties on droplet geometry and growth temperatures in our experiments and, as demonstrated in Sec. V A, does not affect the descriptive and predictive character of the model

(provided the prefactor in the nucleation rate is adjusted accordingly). This rather low value of γ_e might play a part in the preferential formation of ZB in self-catalyzed GaAs NW growth, by making nucleation at the triple phase line unfavorable.[10,23]

Arsenic material balance is a key ingredient of our model. As mentioned earlier, because of the stochastic nature of nucleation, which produces noticeable effects in III-V NW VLS growth due to the low concentration of As in the droplet,[44] this can only hold on average over a time scale at least of the order of the interval between successive nucleation events. It is beyond the scope of this paper to discuss in detail this assumption. Suffices to notice that in the present case, the self-limiting character that manifests itself in many instances of NW growth, seems particularly easy to understand. Indeed, in given growth conditions, any temporary increase (decrease) of the As concentration increases (decreases) the rates of the two processes that deplete the droplet in As, namely nucleation and evaporation, and thus drives back the As concentration to a stationary value.

On the other hand, when the As flux is varied over a large interval (e.g., in our pressure series), the rate of consumption of As varies in an even higher proportion (Sec. III A); since evaporation remains moderate and stoichiometric GaAs is formed, the same happens to the Ga consumption rate. Since the NW radius, and thus presumably the droplet volume, do not change appreciably, the rate of Ga arrival to the droplet must change enormously. The way in which the Ga current (which must occur partly by surface diffusion) adapts itself is beyond the reach of our As-only model and calls for schemes that treat on an equal footing group III and group V atoms.[33] However, the fact that the present model accurately describes actual growth experiments confirms that self-catalyzed GaAs NW growth is largely governed by arsenic. Whether this model may apply to other self-catalyzed systems depends to a great extent on the transferability of the key observations that subtend it, in particular the ineffectivity of group V surface diffusion (which might not hold for Sb) and the absence of radial growth. This remains to be studied.

ACKNOWLEDGMENTS

This work was partly carried out within project INSCOOP ANR-11-NANO-012 of the French Agence nationale de la recherche.

APPENDIX: CHEMICAL POTENTIAL, EQUILIBRIUM PRESSURES, AND FINITE SIZE EFFECTS

1. Chemical potential for infinite phases

We first calculate the difference of chemical potential $\Delta\mu(c_{\mathrm{As}},T)$ per III-V pair between a (Ga, As) liquid of atomic composition c_{As} in As and solid ZB GaAs, at temperature T. Finite size effects will be treated in Appendix A 3. Recall that, in a pure phase, the chemical potential per atom equals the Gibbs free energy per atom. Similarly, since we consider stoichiometric GaAs, the chemical potential of a GaAs pair in GaAs is equal to the Gibbs free energy per pair g_{GaAs}. Hence

$$\begin{aligned}\Delta\mu(c_{\mathrm{As}},T) &= \left[\mu^L_{\mathrm{Ga}}(c_{\mathrm{As}},T) - {}^0\mu^L_{\mathrm{Ga}}(T) + \mu^L_{\mathrm{As}}(c_{\mathrm{As}},T) - {}^0\mu^L_{\mathrm{As}}(T)\right] \\ &\quad + \left[{}^0\mu^L_{\mathrm{Ga}}(T) + {}^0\mu^L_{\mathrm{As}}(T) - g_{\mathrm{GaAs}}(T)\right], \end{aligned} \tag{A1}$$

where $\mu^L_{\mathrm{A}}(c_{\mathrm{As}},T)$ is the chemical potential of element A (Ga or As) in the liquid of composition c_{As} and ${}^0\mu^L_{\mathrm{A}}(T)$ the chemical potential in pure liquid A. All the terms in Eq. (A1) can be evaluated by using published data obtained from experimental phase equilibria using the Calphad method. To evaluate the first bracket in Eq. (A1), we note that

$$\begin{aligned}\mu^L_{\mathrm{Ga}} - {}^0\mu^L_{\mathrm{Ga}} &= \hat{g}^L_m(c_{\mathrm{As}},T) - c_{\mathrm{As}}\frac{\partial \hat{g}^L_m}{\partial c_{\mathrm{As}}} + k_B T\ln(1-c_{\mathrm{As}}), \\ \mu^L_{\mathrm{As}} - {}^0\mu^L_{\mathrm{As}} &= \hat{g}^L_m(c_{\mathrm{As}},T) + (1-c_{\mathrm{As}})\frac{\partial \hat{g}^L_m}{\partial c_{\mathrm{As}}} + k_B T\ln c_{\mathrm{As}}, \end{aligned} \tag{A2}$$

where $\hat{g}^L_m$ is the excess Gibbs energy,[47] i.e., the difference between the free energy of the liquid and the weighted average of those of its pure components. Hence

$$\begin{aligned}&\mu^L_{\mathrm{Ga}}(c_{\mathrm{As}},T) - {}^0\mu^L_{\mathrm{Ga}}(T) + \mu^L_{\mathrm{As}}(c_{\mathrm{As}},T) - {}^0\mu^L_{\mathrm{As}}(T) \\ &\quad = 2\hat{g}^L_m + (1-2c_{\mathrm{As}})\frac{\partial \hat{g}^L_m}{\partial c_{\mathrm{As}}} + k_B T\ln[c_{\mathrm{As}}(1-c_{\mathrm{As}})]. \end{aligned} \tag{A3}$$

$\hat{g}^L_m(c_{\mathrm{As}},T)$ can be approximated by using a first degree Redlich-Kister polynomial:

$$\hat{g}^L_m = c_{\mathrm{As}}(1-c_{\mathrm{As}})\sum_{\nu=0}^{1} {}^\nu L^L_{\mathrm{As,Ga}}(2c_{\mathrm{As}}-1)^\nu, \tag{A4}$$

the T-dependent coefficients ${}^\nu L^L_{\mathrm{As,Ga}}$ of which are given by Ansara *et al.*[47] (see Table II).

The second bracket in Eq. (A1) rewrites

$$\begin{aligned}&{}^0\mu^L_{\mathrm{Ga}}(T) + {}^0\mu^L_{\mathrm{As}}(T) - g_{\mathrm{GaAs}}(T) \\ &\quad = {}^0\mu^L_{\mathrm{Ga}}(T) - {}^0h^S_{\mathrm{Ga}}(T_0) + {}^0\mu^L_{\mathrm{As}}(T) - {}^0h^S_{\mathrm{As}}(T_0) \\ &\qquad - \left[g_{\mathrm{GaAs}}(T) - {}^0h^S_{\mathrm{Ga}}(T_0) - {}^0h^S_{\mathrm{As}}(T_0)\right], \end{aligned} \tag{A5}$$

where ${}^0h^S_{\mathrm{A}}(T_0)$ is the atomic enthalpy of element A in its reference solid structure (orthorhombic for Ga, rhombohedral for As) at temperature $T_0 = 298.15$ K, which is taken as a standard energy reference in the literature.[47,60] To evaluate the right side of Eq. (A5), we use the formulas for ${}^0\mu^L_{\mathrm{A}}(T) - {}^0h^S_{\mathrm{A}}(T_0)$ (A = Ga or As) given by Dinsdale[60] and the formula for $g_{\mathrm{GaAs}}(T) - {}^0h^S_{\mathrm{Ga}}(T_0) - {}^0h^S_{\mathrm{As}}(T_0)$ (scaled for half a mole of GaAs) given by Ansara *et al.*[47] (Table II). This terminates the calculation of the difference of chemical potential between large liquid and solid phases. The variations of $\Delta\mu$ with c_{As} and T are illustrated in Fig. 10.

2. Equilibrium pressures for infinite phases

Let us consider a gas phase at total pressure P containing various species, in particular As_n molecules at partial pressures π_n. Assuming that the gas phase is an ideal solution, the chemical potential of the As_n molecule is

$$\mu^G_{\mathrm{As}_n}(\pi_n,T) = {}^0\mu^G_{\mathrm{As}_n}(T) + k_B T\ln\frac{\pi_n}{P}, \tag{A6}$$

TABLE II. Thermodynamic quantities for use in Eqs. (A4), (A5), (A8), and (A9) and their values in J/mol as a function of temperature T (in K). For use in our calculations, where atomic or molecular quantities are handled, these expressions must be divided by Avogadro's number. The last quantity is given only for the As_2 species and, when substituted in Eq. (A8), gives p_2^∞ in units of 0.1 MPa. When the reference quoted in the third column gives several expressions, only that relative to the temperature range of interest for self-catalyzed GaAs growth is retained.

Quantity	Value	Ref.
${}^0L^L_{\mathrm{As,Ga}}$	$-25503.6 - 4.3109\ T$	47
${}^1L^L_{\mathrm{As,Ga}}$	-5174.7	47
${}^0\mu^L_{\mathrm{Ga}}(T) - {}^0h^S_{\mathrm{Ga}}(T_0)$	$-1389.188 + 114.049043\ T$	
	$-26.0692906\ T \ln T + 0.1506 \times 10^{-3}\ T^2 - 0.040173 \times 10^{-6}\ T^3 - 118332\ T^{-1}$	60
${}^0\mu^L_{\mathrm{As}}(T) - {}^0h^S_{\mathrm{As}}(T_0)$	$17172.453 + 99.78639\ T - 23.3144\ T \ln T - 2.71613 \times 10^{-3}\ T^2 + 11600\ T^{-1}$	60
$g_{\mathrm{GaAs}}(T) - {}^0h^S_{\mathrm{Ga}}(T_0) - {}^0h^S_{\mathrm{As}}(T_0)$	$-104352 + 265.43256\ T - 48.681258\ T \ln T - 0.0011158\ T^2$	
	$+127670\ T^{-1} - 7.1378 \times 10^{-7}\ T^3$	47
${}^0\mu^G_{\mathrm{As_2}}(T) - 2\,{}^0h^S_{\mathrm{As}}(T_0) - k_B T \ln P$	$179351.548 + 10.5519715\ T - 37.35966\ T \ln T - 5.61806 \times 10^{-5}\ T^2$	
	$-2.13098 \times 10^{-8}\ T^3 + 104881.15\ T^{-1}$	47

where ${}^0\mu^G_{\mathrm{As}_n}$ is the corresponding chemical potential in a pure As_n vapor at pressure P and temperature T. The As_n pressure $p_n^\infty(c_{\mathrm{As}}, T)$ in equilibrium with a (Ga, As) liquid with As atomic concentration c_{As} is defined by

$$\mu^G_{\mathrm{As}_n}(p_n^\infty, T) = n\mu^L_{\mathrm{As}}(c_{\mathrm{As}}, T). \tag{A7}$$

From Eqs. (A6) and (A7) we get

$$\begin{aligned} k_B T \ln p_n^\infty &= n\mu^L_{\mathrm{As}}(c_{\mathrm{As}}, T) - {}^0\mu^G_{\mathrm{As}_n}(T) + k_B T \ln P \\ &= n\left[\mu^L_{\mathrm{As}}(c_{\mathrm{As}}, T) - {}^0h^S_{\mathrm{As}}(T_0)\right] \\ &\quad - \left[{}^0\mu^G_{\mathrm{As}_n}(T) - n\,{}^0h^S_{\mathrm{As}}(T_0) - k_B T \ln P\right]. \end{aligned} \tag{A8}$$

The first bracket in Eq. (A8) rewrites

$$\begin{aligned} \mu^L_{\mathrm{As}}(c_{\mathrm{As}}, T) - {}^0h^S_{\mathrm{As}}(T_0) &= \left[\mu^L_{\mathrm{As}}(c_{\mathrm{As}}, T) - {}^0\mu^L_{\mathrm{As}}(T)\right] \\ &\quad + \left[{}^0\mu^L_{\mathrm{As}}(T) - {}^0h^S_{\mathrm{As}}(T_0)\right]. \end{aligned} \tag{A9}$$

In turn, the first bracket in Eq. (A9) is calculated by using Eqs. (A2) and (A4) and the second one by using the expressions given by Dinsdale,[60] as in Appendix A 1 (Table II). As for the second bracket in Eq. (A8), it is found by omitting the pressure-dependent term in the expressions given, for each molecule As_n, by Ansara *et al*. in Appendix II of Ref. 47 (see Table II). This terminates the calculation of the equilibrium pressures p_n^∞ of the As_n molecules for a large liquid phase. The variations of p_2^∞ with c_{As} and T are illustrated in Fig. 10.

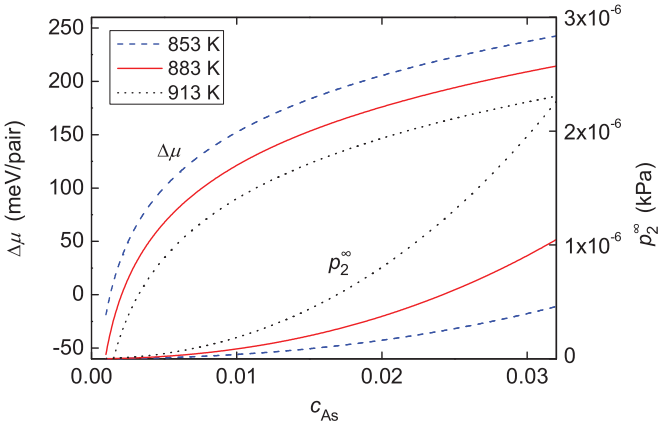

FIG. 10. (Color online) Variation with As concentration in the liquid of the difference of chemical potential $\Delta\mu$ between liquid and solid ZB GaAs and of the equilibrium pressure p_2^∞ of As_2 molecules, for the three temperatures indicated.

3. Finite size effects

First recall the relations between contact angle β, NW radius R, and the radius R_d, surface S_d and volume V_d of the droplet:

$$\begin{aligned} R &= R_d \sin\beta, \\ S_d &= 2\pi R^2 \frac{1 - \cos\beta}{\sin^2\beta}, \\ V_d &= \pi R^3 \frac{(1 - \cos\beta)^2\,(2 + \cos\beta)}{3\sin^3\beta}. \end{aligned} \tag{A10}$$

Two finite size effects must be taken into account. These effects have a common cause, namely the change of the liquid-vapor interface area when a few atoms are added to, or removed from, the nanosize droplet. They modify two of the currents considered in Sec. II. The change of the chemical potential in the liquid [Gibbs-Thomson (GT) effect] modifies the nucleation probability, whereas the elevation of the equilibrium pressure of the various gas species (Kelvin effect) increases evaporation.

The GT effect is usually treated as an increase of the chemical potential in the liquid, since adding an atom to the droplet produces an increase of its external area. However, as discussed in depth by Dubrovskii *et al*.,[52] for VLS growth, a detailed calculation of the nucleation barrier, depending on the location of the nucleus at the LS interface, has to be carried out. Since the critical nucleus typically forms in a time much shorter than the time needed for the external fluxes to replace the atoms transferred from liquid to nucleus, nucleation occurs at a constant total number of atoms in the system. The area of the droplet decreases because atoms are removed from the liquid to form the nucleus; however, in the case considered here (the nucleus forms away from the triple phase line), it also increases because the solid nucleus is entirely embedded in the liquid. The volume of the droplet (i.e., the volume enclosed in its external surface, including the nucleus) also changes. Since the nucleus occupies only a small fraction of the LS interface, the surface and volume changes are not effected by

a change of the NW radius but by a small change of the contact angle β.

Let δS_d and δV_d be the changes of droplet surface and volume when one or a few atoms are added or removed at constant NW radius. By differentiating the expressions of Eq. (A10), we find that $\delta S_d/\delta V_d = 2\sin\beta/R$. Thus, the net change of the difference of chemical potential per pair that intervenes in nucleation is[52]

$$\Delta\mu_{GT} = \frac{2\left(\omega_p^L - \omega_p^S\right)\gamma_{\mathrm{Ga}}^L \sin\beta}{R}, \tag{A11}$$

where ω_p^L and ω_p^S are the volumes of a (Ga, As) pair in the liquid and the solid, respectively, and γ_{Ga}^L the surface energy of liquid Ga (taken as a good approximation of the surface energy of the droplet, which is nearly pure Ga). Contrary to the usual GT effect, $\Delta\mu_{GT}$ may be of either sign.[52] In the case of GaAs, the two pair volumes are very close ($\omega_p^S = 0.04573$ nm^3 and $\omega_p^L = 0.04376$ nm^3 at 900 K, the latter from the atomic volumes in the liquid state[61,62]) and $\Delta\mu_{GT}$ is slightly negative.

As for the Kelvin effect, the evaporation of an As_n molecule reduces the droplet volume by $\delta V_d = n\omega_{\mathrm{As}}^L$, where ω_{As}^L is the atomic volume of As in the liquid. Using the formula for $\delta S_d/\delta V_d$ given above, we find that the chemical potential of the set of n As atoms in the liquid is increased by

$$\Delta\mu_n = \frac{2n\omega_{\mathrm{As}}^L\gamma_{\mathrm{Ga}}^L \sin\beta}{R}. \tag{A12}$$

Inserting the modified $\Delta\mu$ in Eq. (A8) shows that the equilibrium pressure of As_n becomes

$$p_n(c_{\mathrm{As}},T,R) = p_n^{\infty}(c_{\mathrm{As}},T)\exp\left(\frac{\Delta\mu_n}{k_BT}\right). \tag{A13}$$

Since the droplet area decreases upon evaporation, the chemical potential in the liquid and the equilibrium pressure are both augmented with respect to the case of an infinite liquid.

*frank.glas@lpn.cnrs.fr

[1] K. A. Dick, Prog. Cryst. Growth Charac. Mater. **54**, 138 (2008).
[2] M. T. Borgström, M. A. Verheijen, G. Immink, T. de Smet, and E. P. A. M. Bakkers, Nanotechnology **17**, 4010 (2006).
[3] F. Jabeen, G. Patriarche, F. Glas, and J.-C. Harmand, J. Cryst. Growth **323**, 293 (2011).
[4] A. Fontcuberta i Morral, C. Colombo, G. Abstreiter, J. Arbiol, and J. R. Morante, Appl. Phys. Lett. **92**, 063112 (2008).
[5] F. Jabeen, V. Grillo, S. Rubini, and F. Martelli, Nanotechnology **19**, 275711 (2008).
[6] C. Colombo, D. Spirkoska, M. Frimmer, G. Abstreiter, and A. Fontcuberta i Morral, Phys. Rev. B **77**, 155326 (2008).
[7] D. Spirkoska, J. Arbiol, A. Gustafsson, S. Conesa-Boj, F. Glas, I. Zardo, M. Heigoldt, M. H. Gass, A. L. Bleloch, S. Estrade, M. Kaniber, J. Rossler, F. Peiro, J. R. Morante, G. Abstreiter, L. Samuelson, and A. Fontcuberta i Morral, Phys. Rev. B **80**, 245325 (2009).
[8] J. H. Paek, T. Nishiwaki, M. Yamaguchi, and N. Sawaki, Phys. Status Solidi C **6**, 1436 (2009).
[9] B. Bauer, A. Rudolph, M. Soda, A. Fontcuberta i Morral, J. Zweck, D. Schuh, and E. Reiger, Nanotechnology **21**, 435601 (2010).
[10] G. E. Cirlin, V. G. Dubrovskii, Y. B. Samsonenko, A. D. Bouravleuv, K. Durose, Y. Y. Proskuryakov, B. Mendes, L. Bowen, M. A. Kaliteevski, R. A. Abram, and D. Zeze, Phys. Rev. B **82**, 035302 (2010).
[11] P. Krogstrup, R. Popovitz-Biro, E. Johnson, M. H. Madsen, J. Nygård, and H. Shtrikman, Nano Lett. **10**, 4475 (2010).
[12] D. Rudolph, S. Hertenberger, S. Bolte, W. Paosangthong, D. Spirkoska, M. Döblinger, M. Bichler, J. J. Finley, G. Abstreiter, and G. Koblmüller, Nano Lett. **11**, 3848 (2011).
[13] S. Plissard, G. Larrieu, X. Wallart, and P. Caroff, Nanotechnology **22**, 275602 (2011).
[14] T. Rieger, S. Heiderich, S. Lenk, M. I. Lepsa, and D. Grützmacher, J. Cryst. Growth **353**, 39 (2012).
[15] M. R. Ramdani, J. C. Harmand, F. Glas, G. Patriarche, and L. Travers, Cryst. Growth Design **13**, 91 (2013).
[16] M. Heiß, A. Gustafsson, S. Conesa-Boj, F. Peiro, J. R. Morante, G. Abstreiter, J. Arbiol, L. Samuelson, and A. Fontcuberta i Morral, Nanotechnology **20**, 075603 (2009).
[17] J. Paek, M. Yamaguchi, and H. Amano, J. Cryst. Growth **323**, 315 (2011).
[18] R. L. Woo, L. Gao, N. Goel, M. K. Hudait, K. L. Wang, S. Kodambaka, and R. F. Hicks, Nano Lett. **9**, 2207 (2009).
[19] B. Mandl, J. Stangl, E. Hilner, A. A. Zakharov, K. Hillerich, A. W. Dey, L. Samuelson, G. Bauer, K. Deppert, and A. Mikkelsen, Nano Lett. **10**, 4443 (2010).
[20] H. Zhou, M. Pozuelo, R. F. Hicks, and S. Kodambaka, J. Cryst. Growth **319**, 25 (2011).
[21] V. G. Dubrovskii, N. V. Sibirev, G. E. Cirlin, J. C. Harmand, and V. M. Ustinov, Phys. Rev. E **73**, 021603 (2006).
[22] J. Johansson, L. S. Karlsson, C. P. T. Svensson, T. Mårtensson, B. A. Wacaser, K. Deppert, L. Samuelson, and W. Seifert, Nat. Mater. **5**, 574 (2006).
[23] F. Glas, J. C. Harmand, and G. Patriarche, Phys. Rev. Lett. **99**, 146101 (2007).
[24] M. Tchernycheva, L. Travers, G. Patriarche, F. Glas, J.-C. Harmand, G. E. Cirlin, and V. G. Dubrovskii, J. Appl. Phys. **102**, 094313 (2007).
[25] E. J. Schwalbach and P. W. Voorhees, Nano Lett. **8**, 3739 (2008).
[26] M. C. Plante and R. R. LaPierre, J. Appl. Phys. **105**, 114304 (2009).
[27] J. Johansson, L. S. Karlsson, K. A. Dick, J. Bolinsson, B. A. Wacaser, K. Deppert, and L. Samuelson, Cryst. Growth Design **9**, 766 (2009).
[28] V. G. Dubrovskii, N. V. Sibirev, G. E. Cirlin, A. D. Bouravleuv, Y. B. Samsonenko, D. L. Dheeraj, H. L. Zhou, C. Sartel, J. C. Harmand, G. Patriarche, and F. Glas, Phys. Rev. B **80**, 205305 (2009).
[29] K. W. Schwarz and J. Tersoff, Nano Lett. **11**, 316 (2011).
[30] P. Krogstrup, S. Curiotto, E. Johnson, M. Aagesen, J. Nygård, and D. Chatain, Phys. Rev. Lett. **106**, 125505 (2011).
[31] R. E. Algra, M. A. Verheijen, L.-F. Feiner, G. G. W. Immink, W. J. P. van Enckevort, E. Vlieg, and E. P. A. M. Bakkers, Nano Lett. **11**, 1259 (2011).

[32]V. G. Dubrovskii, T. Xu, Y. Lambert, J.-P. Nys, B. Grandidier, D. Stiévenard, W. Chen, and P. Pareige, Phys. Rev. Lett. **108**, 105501 (2012).
[33]P. Krogstrup, H. I. Jørgensen, E. Johnson, M. H. Madsen, C. B. Sørensen, A. Fontcuberta i Morral, M. Aagesen, J. Nygård, and F. Glas, J. Phys. D: Appl. Phys. **46**, 313001 (2013).
[34]K. Hiruma, M. Yasawa, K. Haraguchi, K. Ogawa, T. Katsuyama, M. Koguchi, and H. Kakibayashi, J. Appl. Phys. **74**, 3162 (1993).
[35]S. A. Dayeh, E. T. Yu, and D. Wang, Nano Lett. **7**, 2486 (2007).
[36]M. C. Plante and R. R. LaPierre, Nanotechnology **19**, 495603 (2008).
[37]H. J. Joyce, Q. Gao, H. H. Tan, C. Jagadish, Y. Kim, M. A. Fickenscher, S. Perera, T. B. Hoang, L. M. Smith, H. E. Jackson, J. M. Yarrison-Rice, X. Zhang, and J. Zou, Nano Lett. **9**, 695 (2009).
[38]C. Sartel, D. L. Dheeraj, F. Jabeen, and J. C. Harmand, J. Cryst. Growth **312**, 2073 (2010).
[39]J.-C. Harmand, F. Glas, and G. Patriarche, Phys. Rev. B **81**, 235436 (2010).
[40]M. Koguchi, H. Kakibayashi, M. Yasawa, K. Hiruma, and T. Katsuyama, Jpn. J. Appl. Phys. **31**, 2061 (1992).
[41]S. Paiman, Q. Gao, H. H. Tan, C. Jagadish, K. Pemasiri, M. Montazeri, H. E. Jackson, L. M. Smith, J. M. Yarrison-Rice, X. Zhang, and J. Zou, Nanotechnology **20**, 225606 (2009).
[42]K. A. Dick, P. Caroff, J. Bolinsson, M. E. Messing, J. Johansson, K. Deppert, L. R. Wallenberg, and L. Samuelson, Semicond. Sci. Technol. **25**, 024009 (2010).
[43]H. J. Joyce, J. Wong-Leung, Q. Gao, H. H. Tan, and C. Jagadish, Nano Lett. **10**, 908 (2010).
[44]F. Glas, J. C. Harmand, and G. Patriarche, Phys. Rev. Lett. **104**, 135501 (2010).
[45]F. Glas, J. Appl. Phys. **108**, 073506 (2010).
[46]J. Johansson, C. P. T. Svensson, T. Mårtensson, L. Samuelson, and W. Seifert, J. Phys. Chem. B **109**, 13567 (2005).
[47]I. Ansara, C. Chatillon, H. L. Lukas, T. Nishizawa, H. Ohtani, K. Ishida, M. Hillert, B. Sundman, B. B. Argent, A. Watson, T. Chart, and T. Anderson, Calphad **18**, 177 (1994).
[48]V. G. Dubrovskii, G. E. Cirlin, I. P. Soshnikov, A. A. Tonkikh, N. V. Sibirev, Y. B. Samsonenko, and V. M. Ustinov, Phys. Rev. B **71**, 205325 (2005).
[49]F. Glas, Phys. Status Solidi B **247**, 254 (2010).
[50]N. V. Sibirev, M. Tchernycheva, M. A. Timofeeva, J.-C. Harmand, G. E. Cirlin, and V. G. Dubrovskii, J. Appl. Phys. **111**, 104317 (2012).
[51]M. Knudsen, *The Kinetic Theory of Gases* (Methuen, London, 1950).
[52]V. G. Dubrovskii, N. V. Sibirev, J. C. Harmand, and F. Glas, Phys. Rev. B **78**, 235301 (2008).
[53]C.-Y. Wen, M. C. Reuter, J. Bruley, J. Tersoff, S. Kodambaka, E. A. Stach, and F. M. Ross, Science **326**, 1247 (2009).
[54]A. D. Gamalski, C. Ducati, and S. Hofmann, J. Phys. Chem. C **115**, 4413 (2011).
[55]C.-Y. Wen, J. Tersoff, K. Hillerich, M. C. Reuter, J. H. Park, S. Kodambaka, E. A. Stach, and F. M. Ross, Phys. Rev. Lett. **107**, 025503 (2011).
[56]I. N. Markov, *Crystal Growth for Beginners* (World Scientific, Singapore, 2003).
[57]P. Caroff, K. A. Dick, J. Johansson, M. E. Messing, K. Deppert, and L. Samuelson, Nat. Nanotechnol. **4**, 50 (2008).
[58]A. Li, N. V. Sibirev, D. Ercolani, V. G. Dubrovskii, and L. Sorba, Cryst. Growth Design **13**, 878 (2013).
[59]Y. H. Kim, D. W. Park, and S. J. Lee, Appl. Phys. Lett. **100**, 033117 (2012).
[60]A. T. Dinsdale, Calphad **15**, 317 (1991).
[61]W. H. Hoather, Proc. R. Soc. **48**, 699 (1936).
[62]P. J. McGonigal and A. V. Grosse, J. Phys. Chem. **67**, 924 (1963).